ACS OMEGA

Article

http://pubs.acs.org/journal/acsodf

Fluorescent, Magnetic Multifunctional Carbon Dots for Selective Separation, Identification, and Eradication of Drug-Resistant Superbugs

Avijit Pramanik,[†] Stacy Jones,[†] Francisco Pedraza,[‡] Aruna Vangara,[†] Carrie Sweet,[†] Mariah S. Williams,[†] Vikram Ruppa-Kasani,[†] Sean Edward Risher,[†] Dhiraj Sardar,[‡] and Paresh Chandra Ray*[,†]

[†]Department of Chemistry and Biochemistry, Jackson State University, 1400 J. R. Lynch Street, P.O. Box 17910, Jackson, Mississippi 39217-0510, United States

[‡]Department of Physics and Astronomy, University of Texas at San Antonio, One UTSA Circle, San Antonio, Texas 78249-0697, United States

ABSTRACT: The emergence of drug-resistant superbugs remains a major burden to society. As the mortality rate caused by sepsis due to superbugs is more than 40%, accurate identification of blood infections during the early stage will have a huge significance in the clinical setting. Here, we report the synthesis of red/blue fluorescent carbon dot (CD)-attached magnetic nanoparticle-based multicolor multifunctional CD-based nanosystems, which can be used for selective separation and identification of superbugs from infected blood samples. The reported data show that multifunctional fluorescent magneto-CD nanoparticles are capable of isolating Methicillin-resistant *Staphylococcus aureus* (MRSA) and *Salmonella* DT104 superbug from whole blood samples, followed by accurate identification via multicolor fluorescence imaging. As multidrug-resistant (MDR) superbugs are resistant to antibiotics available in the market, this article also reports the design of antimicrobial peptide-conjugated multicolor fluorescent magneto-CDs for effective separation, accurate identification, and complete disinfection of MDR superbugs from infected blood. The reported data demonstrate that by combining pardaxin antimicrobial peptides, magnetic nanoparticles, and multicolor fluorescent CDs into a single system, multifunctional CDs represent a novel material for efficient separation, differentiation, and eradication of superbugs. This material shows great promise for use in clinical settings.

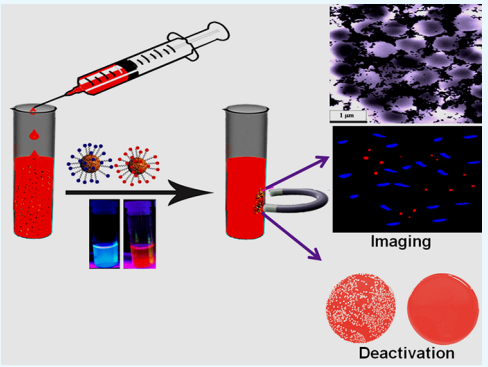

1. INTRODUCTION

Center for Global Health predicts that drug-resistant superbugs kill 700 000 people per year and pose a fundamental threat to human health.[1−4] World Health Organization indicates that by 2050, superbugs could be responsible for 10 million deaths per year, more than the number of people who die from cancer yearly.[1,2] Sepsis due to blood stream infection is one of the major health problems with a mortality rate of more than 40%.[1−3] The high mortality rate is mainly due to the absence of technology available in clinics which can rapidly detect and identify bacteria from clinical blood samples in the early stages of infection.[3−8] The present "gold standard" used in clinics is bacterial blood cultures for 24−48 h and then susceptibility testing for drug resistance.[3−8] The whole process requires several days to obtain accurate results. Because patients need to be treated at the time of the visit, physicians prescribe broad-spectrum antibiotics.[6−12] This general approach not only is inadequate to treat patients who have drug-resistant infections but also encourages antibiotic resistance.[8−14] Owing to the inability of the current methods to provide accurate results in a short time, new technology that can be used to rapidly diagnose drug-resistant superbugs in a point-of-care setting is needed.[1−8] On the basis of this need, this article reports the design of multicolor fluorescent carbon dot (CD)-conjugated magnetic nanoparticle-based multifunctional nanosystem for the selective separation and accurate identification of superbugs from infected blood samples.

Carbon dots (CDs) are quasispherical particles of diameters less than 5 nm, whose surface contains multiple oxygen-containing moieties.[15−30] Because they can be produced from inexpensive starting materials in large scale and exhibit remarkably bright multicolor photoluminescence due to quantum confinement effects, CDs hold great promise for daily-life applications.[31−41] Similarly, magnetic nanoparticles have been used commonly for the magnetic separation of targeted biological molecules from blood.[16,30,42,43] Several recent reports show that the separation of targeted molecules from blood is necessary to minimize light scattering and autofluorescence during imaging.[15,16,30,42,43] In this approach, the magnetic properties of the multifunctional CDs have been

Received: December 18, 2016
Accepted: February 3, 2017
Published: February 15, 2017

DOI: 10.1021/acsomega.6b00518
ACS Omega 2017, 2, 554−562

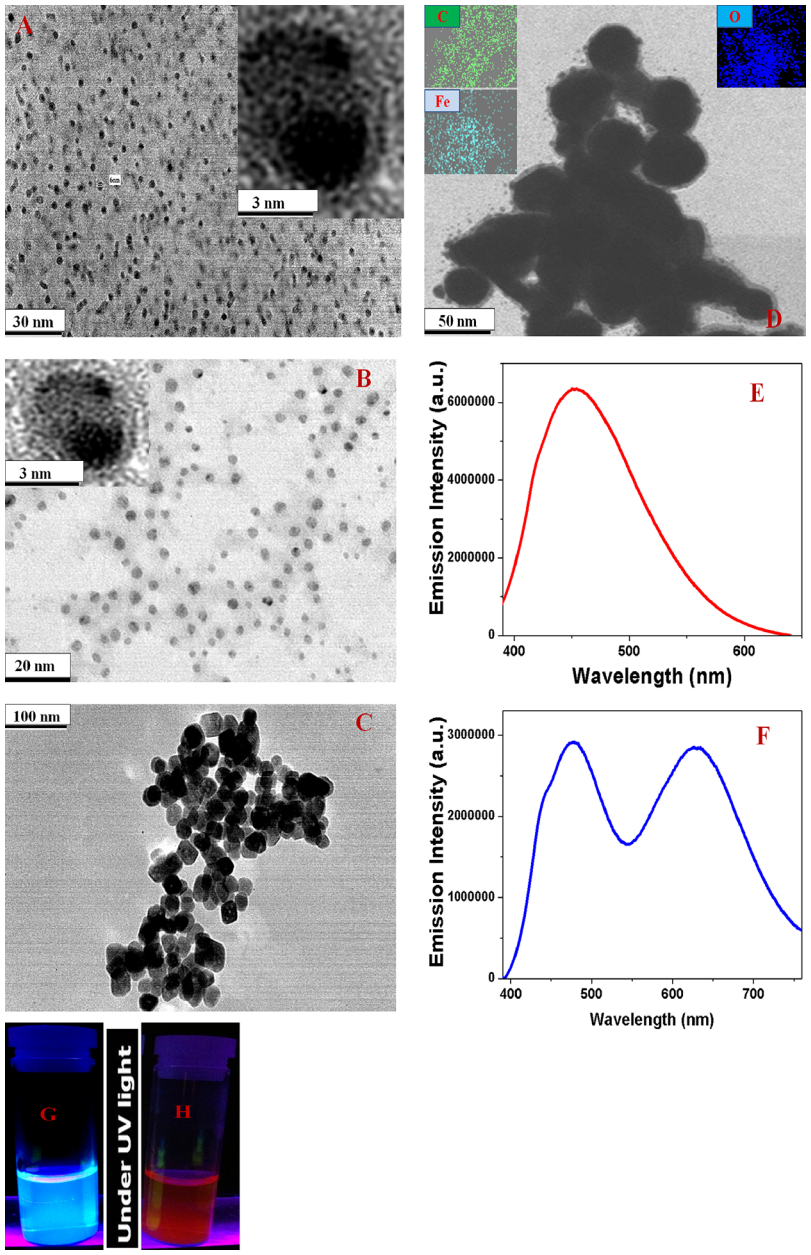

Figure 1. (A) TEM image of freshly prepared blue fluorescent CDs. Inset: HR-TEM image of a single particle. (B) TEM image of freshly prepared red fluorescent CDs. Inset: HR-TEM image of a single particle. (C) TEM image of freshly prepared acid-functionalized magnetic nanoparticles. (D) TEM image of multifunctional magneto-CD nanoparticles. Insets: EDX elemental mapping of Fe, C, and O in magneto-CD nanoparticles. (E) Emission spectra from blue fluorescent magneto-CD-attached nanoparticles at 380 nm excitation. (F) Emission spectra from a mixture of multicolor multifunctional CD-based nanosystems at 380 nm excitation. Blue fluorescent magneto-CD nanoparticles (110 ppm) and red fluorescent magneto-CD nanoparticles (180 ppm) were used for the fluorescence measurement. (G,H) Photograph of multicolor multifunctional CD-based nanosystems in the presence of UV light.

used for the removal of superbugs from the blood sample, providing effective separation and enrichment, a key step in the diagnosis of superbugs in the early stage of an infection. The CDs can be used to visualize different superbugs via multicolor fluorescence imaging to provide accurate diagnosis. To demonstrate that the multifunctional fluorescent magneto-CDs can be used for the analysis of different types of superbugs in a clinical setting, citrated whole blood samples purchased from Colorado Serum Company were inoculated with a trace level of multidrug-resistant (MDR) strains of *Staphylococcus aureus* (MRSA) and *Salmonella enterica* serotype typhimurium definitive phage type 104 (DT104) at different colony-forming unit densities. Experiments have demonstrated that bioconjugated multifunctional fluorescent magneto-CDs are capable of capturing both types of superbugs from the whole blood samples and accurate identification each by multicolor fluorescence imaging.

Because the *Salmonella* DT104 strain is resistant to several antibiotics, including ampicillin, chloramphenicol/florfenicol, spectinomycin/streptomycin, sulfonamides, and tetracyclines, and also no new antibiotics for this superbug has emerged, the development of alternative antimicrobial agents is urgent.[1−8] Antimicrobial peptides are natural and synthetic oligopeptides that are highly promising antimicrobial agents against super-

DOI: 10.1021/acsomega.6b00518
ACS Omega 2017, 2, 554−562

bugs by bolstering the host's defense and modulating the immune response.[8−13,38−40] Pardaxin (Gly-Phe-Phe-Ala-Leu-Ile-Pro-Lys-Ile-Ile-Ser-Ser-Pro-Leu-Phe-Lys-Thr-Leu-Leu-Ser-Ala-Val-Gly-Ser-Ala-Leu-Ser-Ser-Ser-Gly-Gly-Gln-Glu) is a well-documented pore-forming peptide with antimicrobial activity against both Gram-positive and Gram-negative bacteria through the disruption of bacterial membranes and the arachidonic acid cascade.[12,13] By combining pardaxin antimicrobial peptides, magnetic nanoparticles, and multicolor fluorescent CDs into a single system, the multifunctional CDs represent a novel material for total separation, complete differentiation, and accurate identification of superbugs.

2. RESULTS AND DISCUSSION

2.1. Design of Blue and Red Fluorescent Carbon Dots Using Phenylenediamine. CDs exhibiting strong blue fluorescence were synthesized by hydrothermal heating of *meta*-phenylenediamine in ethanol using a reported method.[26] Similarly, the red fluorescent CDs were synthesized by microwave-assisted heating of *para*-phenylenediamine using a reported method.[26] The experimental details are described in the Methods. Following the synthesis, we purified the particles using silica column chromatography and then characterized them using high-resolution transmission electron microscopy (HR-TEM). We have also used dynamic light scattering (DLS) to determine the size in solution. Freshly prepared blue fluorescent CDs are ∼6 nm in diameter, as shown in the HR-TEM image in Figure 1A.

2.2. Synthesis and Characterization of Blue/Red Fluorescent Magneto-CD Nanoparticles. For the development of multicolor multifunctional CD-based nanosystems, initially we synthesized carboxylic acid-functionalized magnetic nanoparticles using coprecipitation method from ferric chloride and 1,6-hexanedioic acid, as we reported before[15,16,30] and as shown in Schemes 1 and 2. The black Fe_3O_4 nanoparticle precipitate was separated from the supernatant using a neodymium magnet and thoroughly washed several times with water. Fe_3O_4 nanoparticles were characterized using HR-TEM and DLS.

Scheme 1. (A) Synthetic Route for the Development of Blue Fluorescent Carbon Dot-Attached Magnetic Nanoparticle-Based Hybrid Nanomaterials. (B) Synthetic Route for the Development of Anti-*Salmonella*-Antibody-Attached Blue Fluorescent Hybrid Nanomaterials

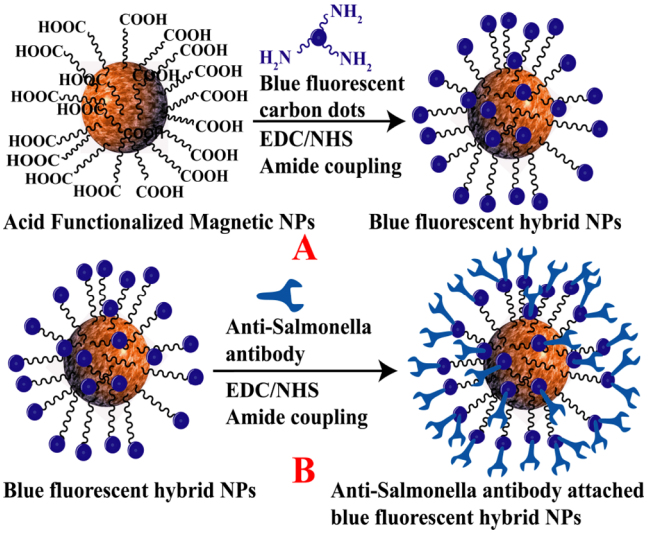

Scheme 2. (A) Synthetic Route for the Development of Red Fluorescent Carbon Dot-Attached Magnetic Nanoparticle-Based Hybrid Nanomaterials. (B) Synthetic Route for the Development of Anti-MRSA-Antibody-Attached Red Fluorescent Hybrid Nanomaterials

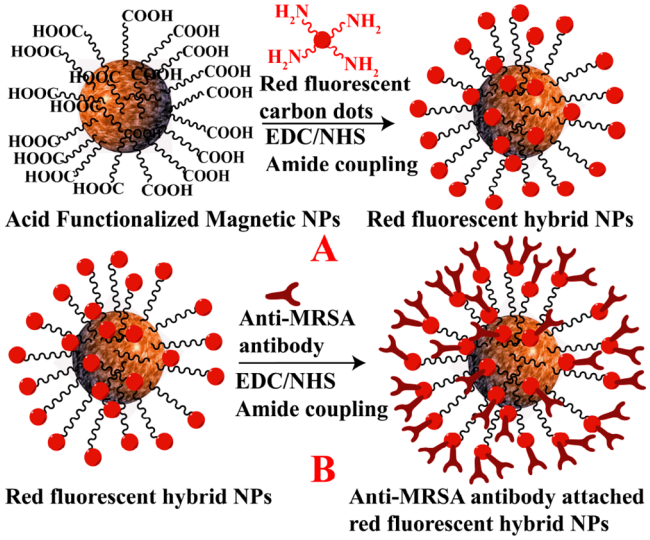

The resultant HR-TEM image is shown in Figure 1C; particles have an average size of about ∼40 nm. DLS results reported in Table 1 also indicate that an average size is of 40 ± 5 nm for magnetic nanoparticles. Superparamagnetic properties were measured using a SQUID magnetometer, which indicates a specific saturation magnetization of 41.8 emu g^{-1} for the magnetite nanoparticles we developed. In the next step, 1-ethyl-3-(3-dimethylaminopropyl)-carbodiimide (EDC)-mediated esterification was used to produce magnetic nanoparticles attached with blue-red fluorescent CDs, as we have reported before.[15] The final product, amide-coupled blue/red fluorescent CD−Fe_3O_4 nanoparticles, was separated using a magnet and washed several times with water to remove the excess CDs. HR-TEM, elemental mapping by energy-dispersive X-ray (EDX) spectroscopy, elemental mapping, and DLS results are reported in Figure 1 and Tables 1 and 2. Figure 1D shows the HR-TEM image for ∼55 nm-diameter purified blue fluorescent magneto-CD nanoparticles. It is noteworthy to observe that multifunctional CD-based nanosystems are about 15 nm larger than the unreacted magnetic nanoparticles. The EDX data shown in Figure 1D indicate the presence of iron, carbon, and oxygen in multifunctional CD-based nanosystems. The DLS data reported in Table 1 confirm a size of about 55 nm for blue fluorescent multifunctional CD-based nanosystems and 50 nm

Table 1. Size Distribution for Blue Fluorescent CDs, Acid-Functionalized Magnetic Nanoparticles, and Multifunctional CD-Based Nanosytems

nanoparticle description	size measured by DLS (nm)	size measured by SEM (nm)
blue fluorescent CDs	6 ± 3	6 ± 3
acid-functionalized magnetic nanoparticles	40 ± 7	40 ± 5
blue fluorescent magneto-CD nanoparticles	55 ± 10	55 ± 8

DOI: 10.1021/acsomega.6b00518
ACS Omega 2017, 2, 554−562

Table 2. Size Distribution for Red Fluorescent CDs, Acid-Functionalized Magnetic Nanoparticles, and Magneto-Red Fluorescent CD Nanoparticles

nanoparticle description	size measured by DLS (nm)	size measured by SEM (nm)
red fluorescent CDs	4 ± 2	4 ± 2
acid-functionalized magnetic nanoparticles	40 ± 7	40 ± 5
red fluorescent magneto-CD nanoparticles	50 ± 8	50 ± 8

for red fluorescent magneto-CD nanoparticles. We determined superparamagnetic properties using the SQUID magnetometer, which indicate a specific saturation magnetization of 38.8 emu g^{-1} for the red magneto-CD nanoparticles and 36.2 emu g^{-1} for the blue magneto-CD nanoparticles.

Figure 1G,H shows the emission spectra from multicolor multifunctional CD-based nanosystems at 380 nm excitation. Experimental data indicate λ_{max} of emission for blue fluorescent magneto-CD nanoparticles of around 462 nm and around 630 nm for red fluorescent magneto-CD nanoparticles. We used quinine sulfate as a standard (QY 54%) for the measurement of photoluminescence quantum yield (QY) for magneto-fluorescent CDs using our reported method.[13−16] Equation 1 was used to calculate the QY for blue fluorescent magneto-CD nanoparticles[14−26]

$$\Phi = \Phi_{ref} \frac{I_{mcd}}{I_{ref}} \frac{A_{ref}}{A_{mcd}} \frac{\eta_{ref}^2}{\eta_{mcd}^2} \quad (1)$$

where the blue fluorescent magneto-CD nanoparticle is termed "mcd" and the quinine sulfate, which was used as the standard, is termed "ref". The photoluminescence QY is denoted as Φ, and the absorbance, fluorescence intensity, and refractive index are denoted as A, I, and η, respectively. Using experimental results and eq 1, the QYs for blue fluorescent CD and blue fluorescent magneto-CD nanoparticles were determined to be 0.51 and 0.28 at 380 nm excitation. Similarly, the QYs for red fluorescent CD and red fluorescent magneto-CD nanoparticles were determined to be 0.24 and 0.12 at 380 nm excitation.

Figure 1G shows that the multicolor multifunctional CD-based nanosystems exhibit blue and red fluorescence, when excited at 380 nm UV light. Consequently, selective and simultaneous targeted imaging of drug-resistant MRSA and *Salmonella* DT104 is possible using magneto-CD nanosystems.

2.3. Developing Antibody-Conjugated Blue-Red Fluorescent Magneto-CD Nanoparticles. For selective binding, separation, and luminescence imaging of *Salmonella* DT104, we have developed anti-*Salmonella*-antibody-attached blue fluorescent magneto-CD nanoparticles. To accomplish this, we have developed amine-conjugated polyethylene glycol (NH_2−PEG)-attached blue fluorescent magneto-CD nanoparticles and then *Salmonella* DT104-targeted antibody was attached with blue fluorescent magneto-CD nanoparticles, utilizing our reported method.[14,15,30] As shown in Scheme 1B, we have used EDC/N-hydroxysuccinimide (NHS) chemistry for the formation of covalent bonds between the carboxyl groups of PEG and the primary amine groups of anti-MRSA antibody. Similarly, for selective binding and imaging of MRSA, we have developed anti-MRSA-antibody-attached red fluorescent magneto-CD nanoparticles using the above procedure. In this case, we have first developed PEG-coated red fluorescent magneto-CD nanoparticles and anti-MRSA antibody was then attached to the hybrid nanoparticle via EDC/NHS chemistry, as shown in Scheme 2B.

2.4. Determining the Possible Nanotoxicity and Photostability. To determine the possible nanotoxicity from our synthesized nanoprobes, we have determined the biocompatibility of the antibody-attached blue fluorescent magneto-CD nanoparticles. For this purpose, around 18 000 CFU/mL *Salmolella* DT104, MRSA, and *Escherichia coli* bacteria were incubated separately with antibody-attached blue fluorescent magneto-CD nanoparticles for 24 h. Similarly, 1.2×10^5 cells/mL normal skin HaCaT cells were incubated separately with antibody-attached multifunctional CD-based nanosystems for 24 h. In the next step, the number of live cells was counted using the colony-counting method[37,39,40] for bacteria and MTT test[14−16] for HaCaT cell lines. Figure 2A shows excellent biocompatibility for the multicolor multifunctional CD-based nanosystems, where more than 97% of bacteria or HaCaT cells are alive after one day of incubation.

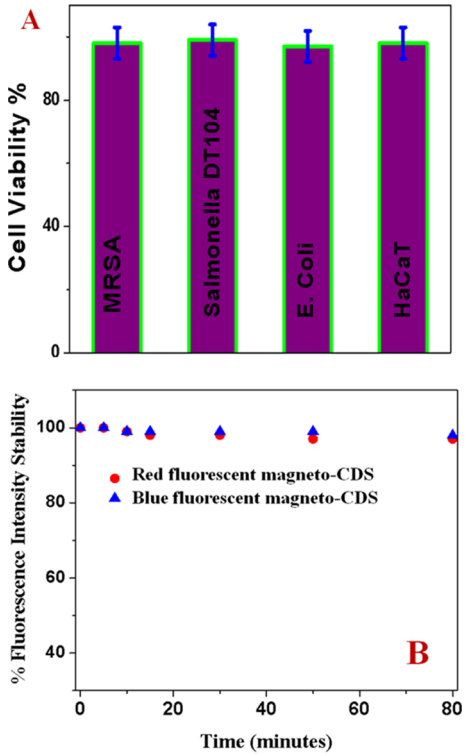

Figure 2. (A) Viability of cells treated with blue fluorescent CDs. (B) Fluorescence intensity for anti-MRSA-antibody-attached blue-red fluorescent CD nanoparticles as a function of time.

To determine the photostability of our synthesized multicolor multifunctional CD-based nanosystems, time-dependent luminescence experiments have been performed using 380 nm excitation for around 1.5 h exposure. Figure 2B indicates excellent photostability for red-blue fluorescent magneto-CD nanoparticles remain, where the luminescence intensity changed only less than 5% even more than 1 h of exposure to light.

2.5. Capturing and Identifying *Salmonella* DT104 and MRSA from Infected Blood. To determine whether multicolor multifunctional CD-based nanosystems could be used for capturing and imaging *Salmonella* DT104 and MRSA superbugs separately and together from the infected sample,

DOI: 10.1021/acsomega.6b00518
ACS Omega 2017, 2, 554−562

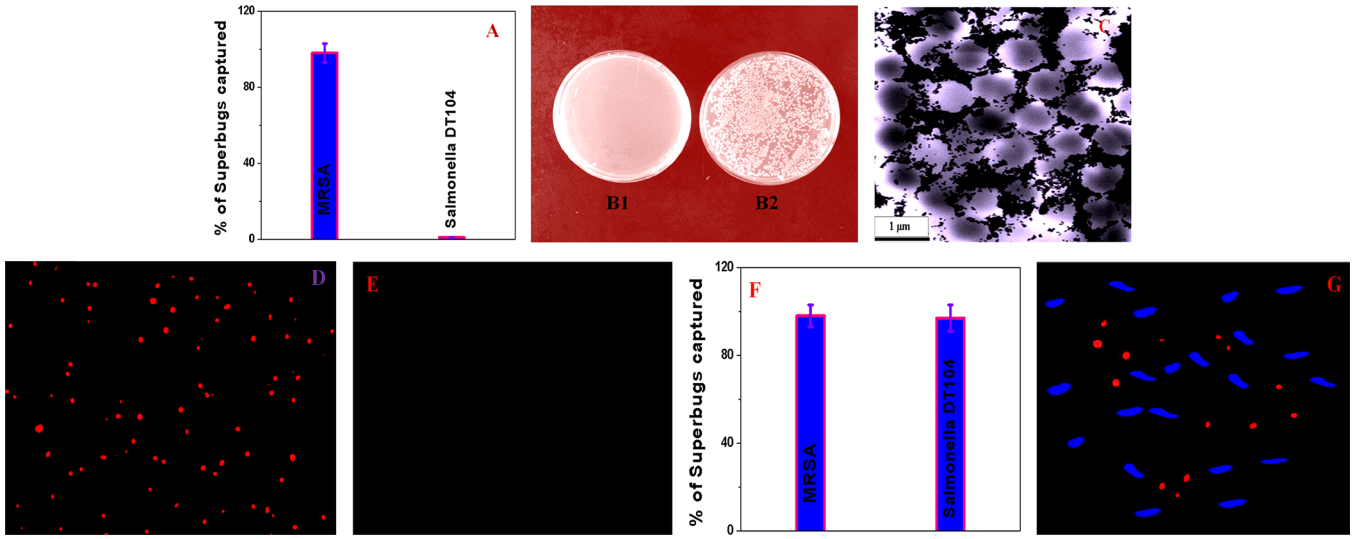

Figure 3. (A) Bar graph of MRSA removal efficiency using anti-MRSA-antibody-attached red fluorescent magneto-CD nanoparticles. (B1,B2) Agar plates of live MRSA bacteria: (B1) before and (B2) after magnetic separation. (C) TEM image of MRSA capture by anti-MRSA-antibody-attached blue fluorescent magneto-CD nanoparticles. (D) Luminescence image of captured MRSA superbugs by anti-MRSA-antibody-attached nanoprobes. (E) Luminescence image from supernatant after magnetic separation. (F) Bar graph of MRSA and *Salmonella* DT104 removal efficiency using both anti-MRSA-antibody-attached red fluorescent magneto-CD nanoparticles and anti-*Salmonella* blue fluorescent magneto-CD nanoparticles. (G) Luminescence image of MRSA and *Salmonella* superbugs after capture by the two nanoprobes.

10^3 CFU/mL of superbugs were injected into 10 mL of citrated whole rabbit blood.

Then, 10^6 cells/mL peripheral blood mononuclear cells (PBMCs) were added into the mixture, which was gently shaken for over 90 min. The mixture was used as an infected blood sample for separation and imaging. Then, different concentrations of anti-MRSA-antibody-attached red fluorescent magneto-CD nanoparticles were added to the infected blood sample and mixed continuously for half an hour. In the next step, targeted MRSA-bound magneto-CD nanoparticles were separated from infected blood using a magnet. Finally, we used reverse transcription polymerase chain reaction (RT-PCR) technique, colony plating technique, and fluorescence mapping analysis[15,30,37−39] to determine the percentage of superbugs that were captured, as reported in Figure 3. The RT-PCR data reported in Figure 3A indicate that around 100% of the MRSA was captured by the magneto-CD we developed. The colony-plating data reported in Figure 3B also indicate complete capture of superbugs. Figure 3C shows the TEM image, which indicates that magneto-CD nanoparticles are attached on the surface of MRSA. In Figure 3D, the red fluorescence image of MRSA superbugs indicates that bioconjugated magnetic-CD nanoparticles are capable of identifying MRSA. Figure 3E shows that the anti-MRSA-antibody-attached red fluorescent magneto-CD nanoparticles do not conjugate with different cells that are present in the infected blood. This lack of binding resulted in no luminescence image for the supernatant following magnetic separation. The above-reported data indicate that anti-MRSA-antibody-conjugated red fluorescent magneto-CD nanoparticles can be used to separate and identify MRSA superbugs from the infected sample.

To determine the selectivity for superbug capturing and identification of MRSA superbugs, the same experiment was performed using *Salmonella* DT104 superbug at different concentrations. As reported in Figure 3A, our experimental data indicate that anti-MRSA-antibody-conjugated red fluorescent magneto-CD nanoparticles are highly selective for MRSA. Thus, *Salmonella* DT104 superbug capture efficiency was less than 1%.

Next, to understand how versatile multicolor fluorescent magneto-CD nanoparticles are for simultaneous capturing of MRSA and *Salmonella* DT104 superbugs, experiments with spiked blood samples containing both MRSA and *Salmonella* DT104 were performed. In this case, 10^3 CFU/mL MRSA and 10^3 CFU/mL *Salmonella* DT104 were infected in the whole blood sample containing 1 million PBMCs. For separation and identification of both MRSA and *Salmonella* DT104 at the same time, anti-MRSA-antibody-attached red fluorescent magneto-CD nanoparticles and anti-*Salmonella*-antibody-attached blue fluorescent magneto-CD nanoparticles were added together in 10 mL of the infected blood sample. Figure 3F shows the RT-PCR data, which indicate that the multicolor multifunctional nanoprobes can be used for more than 98% separation of different superbugs from the infected sample. Figure 3G shows the multicolor luminescence image that reveals that anti-MRSA-antibody-attached red fluorescent magneto-CD nanoparticles and anti-*Salmonella*-antibody-attached blue fluorescent magneto-CD nanoparticles together can be used for the simultaneous identification of MRSA and *Salmonella* DT104. In the reported multicolor luminescence data, the red fluorescent superbug images are MRSA and blue fluorescent superbug images are *Salmonella* DT104. The reported data clearly support the premise that different antibodies-attached multicolor fluorescent magneto-CD nanoparticles can be used for capturing MRSA and *Salmonella* DT104 superbugs selectively and simultaneously from infected whole blood. Although we have shown that anti-*Salmonella*-antibody-conjugated blue fluorescent nanoparticles can be used for the separation and imaging of *Salmonella* DT104, because selectivity is highly dependent on anti-*Salmonella* antibody, it may not be able to separate *Salmonella* DT104 from a mixture of other closely related *Salmonella* strains such as *Salmonella typhimurium*. Similarly, anti-MRSA-antibody-conjugated red fluorescent nanoparticles may not be able to separate MRSA

DOI: 10.1021/acsomega.6b00518
ACS Omega 2017, 2, 554−562

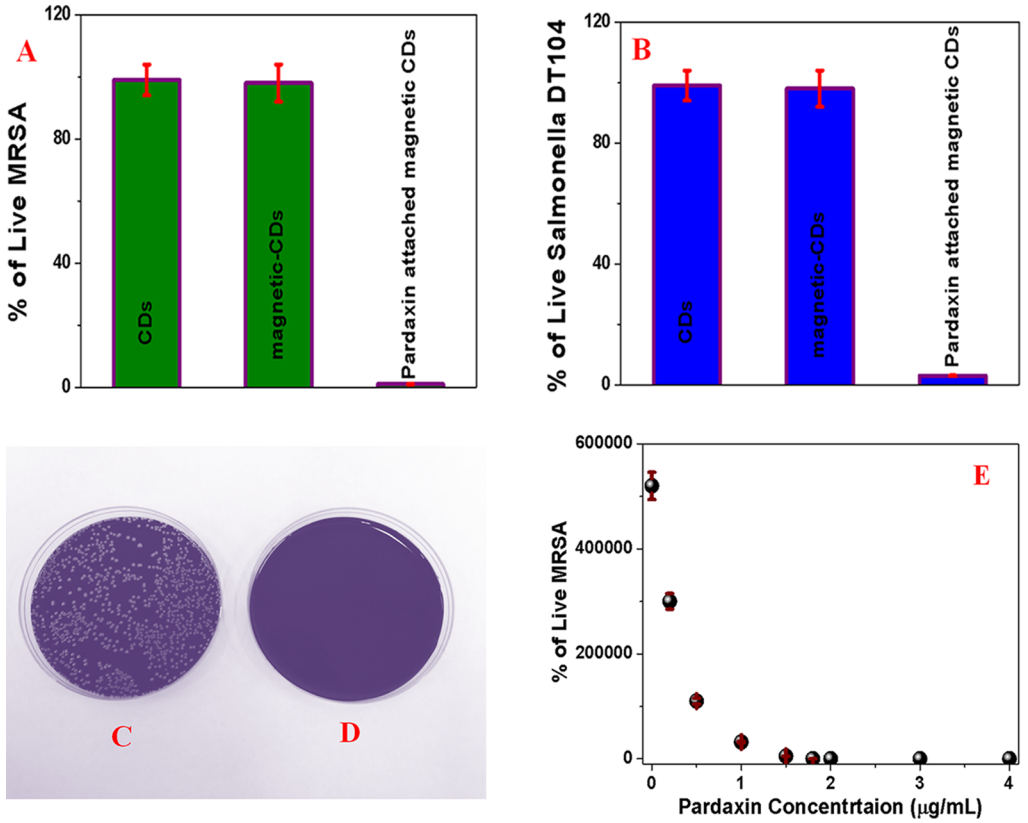

Figure 4. (A) Percentage of live MRSA, when superbugs are captured by (i) anti-MRSA-antibody-attached fluorescent CD nanoparticles, (ii) anti-PSMA-antibody-attached fluorescent magneto-CD nanoparticles, and (iii) pardaxin-conjugated anti-PSMA-antibody-attached fluorescent magneto-CD nanoparticles. (B) Percentage of colonies of *Salmonella* DT104 compared with the control after capture by (i) anti-*Salmonella*-antibody-attached fluorescent CD nanoparticles, (ii) anti-*Salmonella*-antibody-attached fluorescent magneto-CD nanoparticles, and (iii) pardaxin-conjugated anti-*Salmonella*-antibody-attached fluorescent magneto-CD nanoparticles. (C,D) Agar plates of superbugs incubated (C) after being captured by a mixture of anti-MRSA-antibody-attached red fluorescent magneto-CD nanoparticles and anti-*Salmonella*-antibody-attached blue fluorescent magneto-CD nanoparticles and (D) after being captured by a mixture of pardaxin antimicrobial peptides-conjugated anti-MRSA-antibody-attached red fluorescent magneto-CD nanoparticles and pardaxin antimicrobial peptide-conjugated anti-*Salmonella*-antibody-attached blue fluorescent magneto-CD nanoparticles. (E) Plot shows how the percentage of live MRSA varies with the dosage level of pardaxin antimicrobial peptides.

from the mixture of other closely related *Staphylococcus* strains such as *Staphylococcus aureus*.

2.6. Targeted Capturing and Killing of *Salmonella* DT104 and MRSA. Because MRSA and *Salmonella* DT104 superbugs are resistant to several antibiotics, pardaxin antimicrobial peptide-conjugated anti-MRSA-antibody-attached red fluorescent magneto-CD nanoparticles and pardaxin antimicrobial peptide-conjugated anti-*Salmonella*-antibody-attached blue fluorescent magneto-CD nanoparticles were developed. For this purpose, amine groups of pardaxin antimicrobial peptides were attached to the acid-functionalized magnetic nanoparticle using EDC/NHS cross-linking via amide linkage. To determine whether the superbugs captured by antimicrobial peptide-conjugated fluorescent magneto-CD nanoparticles are alive or dead, magnetically separated particles were washed with water and then colony-counting technique was used to determine the percentage of live superbugs. Sample experiments in the absence of antimicrobial peptide conjugation were performed. As shown in Figure 4A–D, almost 100% of MRSA and *Salmonella* were killed when pardaxin antimicrobial peptide-conjugated fluorescent magneto-CD nanoparticles were used.

On the other hand, more than 98% of superbugs were alive when pardaxin antimicrobial peptides are not conjugated with fluorescent magneto-CD nanoparticles. The observed very high killing efficiency of pardaxin antimicrobial peptide-conjugated fluorescent magneto-CD nanoparticles can be due to several facts. It is now well-documented that pore-forming peptides such as pardaxin exhibit great cytotoxicity against Gram-positive and Gram-negative bacteria.[12,13] It is also reported that pardaxin is capable of elevating caspase-3/7 activities and disruption of the mitochondrial membrane potential.[12,13] Pardaxin is also capable for accumulation of reactive oxygen species production.[12,13] All above-described mechanisms are responsible for the death of superbugs in the presence of pardaxin antimicrobial peptide-conjugated fluorescent magneto-CDs nanoparticles. To understand the limit of dosage of the antimicrobial peptide to eradicate MRSA and *Salmonella* DT104 superbugs, we performed pardaxin concentration-dependent study, as reported in Figure 4E, which indicates that 1.8 μg/mL pardaxin is necessary to kill 100% of MRSA. A similar experiment was performed for *Salmonella* DT104, and we found that 2.4 μg/mL pardaxin is necessary to kill 100% of *Salmonella* DT.

3. CONCLUSIONS

In conclusion, this article reports the development of multicolor fluorescent CD-conjugated magnetic nanoparticles that are capable of selective separation and accurate identification of superbugs from infected blood. The new

DOI: 10.1021/acsomega.6b00518
ACS Omega 2017, 2, 554–562

means of capturing and identifying MRSA and *Salmonella* DT104 superbugs from clinically relevant samples is clearly demonstrated. The reported data show that multicolor multifunctional CD-based nanosystems are capable of isolating MRSA and *Salmonella* DT104 superbugs from whole blood samples, followed by accurate identification via multicolor fluorescence imaging. Although we have shown that anti-*Salmonella*-antibody-conjugated blue fluorescent nanoparticles can be used for *Salmonella* DT104 imaging and anti-MRSA-antibody-conjugated red fluorescent nanoparticles can be used for MRSA imaging, we can use either blue or red fluorescent nanoparticles to image MRSA/*Salmonella* or other superbugs, just by changing the specific recognition unit such as antibody. Because multidrug-resistant superbugs are resistant to the antibiotics available in the market, the design of pardaxin antimicrobial peptide-attached multicolor fluorescent magneto-CDs for effective separation, accurate identification, and complete disinfection of MDR superbugs from infected blood is also reported. The reported data indicate that by combining pardaxin antimicrobial peptides with fluorescent magneto-CD nanoparticles, one can develop a novel multifunctional material that has great potential to be used for the identification of MDRB infection in clinics.

4. METHODS

All chemicals including *meta*-phenylenediamine, *para*-phenylenediamine, ethanol, CH_2Cl_2 and MeOH, $NaBH_4$, NH_2−PEG, $FeCl_3{\cdot}6H_2O$, and 1,6-hexanedioic acid were purchased from Fisher Scientific and Sigma-Aldrich. Superbugs, such as multidrug-resistant *Salmonella* DT104 and MRSA, and growth media were purchased from the American Type Culture Collection (ATCC, Rockville, MD).

4.1. Development of Blue Fluorescent Carbon Dots Using *meta*-Phenylenediamine. Blue fluorescent CDs were synthesized by hydrothermal heating of *meta*-phenylenediamine in ethanol using a reported method,[26] as shown in Scheme 1. In brief, 0.9 g of *meta*-phenylenediamine was dissolved in 90 mL of ethanol. Then, the mixture was heated in an autoclave at 180 °C for 12 h. After that, the gray-colored blue fluorescent CDs were then further purified using silica column chromatography using CH_2Cl_2 and MeOH (1:1) as eluants. Yield: 0.09 g, 10%.

4.2. Development of Red Fluorescent Carbon Dots Using *para*-Phenylenediamine. The red fluorescent CDs were synthesized by microwave-assisted heating of *para*-phenylenediamine using a reported method,[26] as shown in Scheme 2. In brief, 0.027 g of *para*-phenylenediamine was dissolved in 50 mL of ethanol, and the mixture was heated for 60 min using a domestic microwave oven (900 W). During this process, a mixture of ethanol and water (1:1) was added into the flask continuously. After that, the resultant solution was dried by solvent evaporation and further purified by silica column chromatography using a mixture of ethanol and ethyl acetate (1:1) as eluants. Yield: 0.014 g, 50%.

4.3. Design of Carboxylic Acid-Conjugated Fe_3O_4 Nanoparticles. We designed carboxylic acid-functionalized Fe_3O_4 magnetic nanoparticles using the co-precipitation method using ferric chloride and 1,6-hexanedioic acid, as we reported before[15,16,30] and as shown in Scheme 1. details were reported before.[15,16,30] At the end, Fe_3O_4 nanoparticles were separated from the supernatant using a magnet.

4.4. Design of Blue-Red Fluorescent Magneto-CD Nanoparticles. For the covalent attachment of blue-red fluorescent magneto-CDs with acid-functionalized magnetic nanoparticles, EDC-mediated esterification was used, as we reported before.[15] The final product, amide-coupled blue-red fluorescent CD−Fe_3O_4 nanoparticles, was separated using a magnet and washed several times with water to remove the excess CDs.

4.5. Development of Antibody-Conjugated Fluorescent Magnetic Nanoprobes. For selective binding, separation, and luminescence imaging of *Salmonella* DT104, we developed an anti-*Salmonella*-antibody-attached blue fluorescent magneto-CD nanoparticles. To accomplish this, we developed amine-conjugated polyethylene glycol (NH_2−PEG)-attached blue fluorescent magneto-CD nanoparticles, and then *Salmonella* DT104-targeted antibody was attached with blue fluorescent magneto-CD nanoparticles, utilizing our reported method.[14,15,30] As shown in Scheme 1B, we used EDC/NHS chemistry for the formation of covalent bonds between carboxyl groups of PEG and primary amine groups of anti-MRSA antibody. Similarly, for selective binding and imaging of MRSA, we developed anti-MRSA-antibody-attached red fluorescent magneto-CD nanoparticles using the above-mentioned procedure. In this case, we first developed PEG-coated red fluorescent magneto-CD nanoparticles, and then anti-MRSA antibody was attached to the hybrid nanoparticle via EDC/NHS chemistry, as shown in Scheme 2B.

4.6. Development of Pardaxin Antimicrobial Peptide-Conjugated Hybrid Nanomaterials. Because MRSA and *Salmonella* DT104 superbugs are resistant to several antibiotics, pardaxin antimicrobial peptide-conjugated anti-MRSA-antibody-attached red fluorescent magneto-CD nanoparticles and pardaxin antimicrobial peptide-conjugated anti-*Salmonella*-antibody-attached blue fluorescent magneto-CD nanoparticles were developed. For this purpose, amine groups of pardaxin antimicrobial peptides were attached to the acid-functionalized magnetic nanoparticle using EDC/NHS cross-linking via amide linkages.

4.7. Superbug Sample Preparation. *Salmonella* DT104 and MRSA were purchased from the ATCC and then cultured according to the ATCC protocol, as we reported before.[37,39,40] For the preparation of infected blood sample, different concentrations of *Salmonella* DT104 and MRSA were prepared by diluting the stock solution.

4.8. Multicolor Luminescence Imaging of Captured Superbugs. For the fluorescence imaging of *Salmonella* DT104 and MRSA superbugs, we used an Olympus IX71 inverted confocal fluorescence microscope fitted with a SPOT Insight digital camera, as we reported before.[14−16,30]

4.9. Finding the Percentage of Live Superbugs. After being magnetically captured, *Salmonella* DT104 and MRSA superbugs were transferred to colony-countable plates and incubated for 1 day. The percentage of live superbugs was determined using a colony counter (Bantex, model 920 A).

AUTHOR INFORMATION

Corresponding Author

*E-mail: paresh.c.ray@jsums.edu. Fax: +16019793674 (P.C.R.).

ORCID

Paresh Chandra Ray: 0000-0001-5398-9930

Notes

The authors declare no competing financial interest.

DOI: 10.1021/acsomega.6b00518
ACS Omega 2017, 2, 554−562

■ ACKNOWLEDGMENTS

Dr. Ray thanks NSF-PREM grant # DMR-1205194, NSF CREST grant # 1547754, NSF RISE grant # 1547836, and NIH RCMI grant (# G12RR013459-13) for generous funding.

■ REFERENCES

(1) World Health Organization. *Antimicrobial Resistance: Global Report on Surveillance 2014*; WHO, 2014.
(2) http://www.who.int/mediacentre/factsheets/fs194/en/ (accessed Dec 8, 2016).
(3) https://www.cdc.gov/drugresistance/ (accessed Dec 8, 2016).
(4) Wang, L.-S.; Gupta, A.; Rotello, V. M. Nanomaterials for the Treatment of Bacterial Biofilms. *ACS Infect. Dis.* **2016**, *2*, 3−4.
(5) Lam, S. J.; O'Brien-Simpson, N. M.; Pantarat, N.; Sulistio, A.; Wong, E. H. H.; Chen, Y.-Y.; Lenzo, J. C.; Holden, J. A.; Blencowe, A.; Reynolds, E. C.; Qiao, G. G. Combating multidrug-resistant Gram-negative bacteria with structurally nanoengineered antimicrobial peptide polymers. *Nat. Microbiol.* **2016**, *1*, 16162.
(6) Li, X.; Robinson, S. M.; Gupta, A.; Saha, K.; Jiang, Z.; Moyano, D. F.; Sahar, A.; Riley, M. A.; Rotello, V. M. Functional Gold Nanoparticles as Potent Antimicrobial Agents Against Multi-Drug-Resistant Bacteria. *ACS Nano* **2014**, *8*, 10682−10686.
(7) Zhang, X.; Chen, X.; Yang, J.; Jia, H.-R.; Li, Y.-H.; Chen, Z.; Wu, F.-G. Quaternized Silicon Nanoparticles with Polarity-Sensitive Fluorescence for Selectively Imaging and Killing Gram-Positive Bacteria. *Adv. Funct. Mater.* **2016**, *26*, 5958−5970.
(8) Bodelón, G.; Montes-García, V.; López-Puente, V.; Hill, E. H.; Hamon, C.; Sanz-Ortiz, M. N.; Rodal-Cedeira, S.; Costas, C.; Celiksoy, S.; Pérez-Juste, I.; Scarabelli, L.; La Porta, A.; Pérez-Juste, J.; Pastoriza-Santos, I.; Liz-Marzán, L. M. Detection and Imaging of Quorum Sensing in *Pseudomonas aeruginosa* Biofilm Communities by Surface-Enhanced Resonance Raman Scattering. *Nat. Mater.* **2016**, *15*, 1203−1211.
(9) Hilchie, A. L.; Wuerth, K.; Hancock, R. E. W. Immune modulation by multifaceted cationic host defense (antimicrobial) peptides. *Nat. Chem. Biol.* **2013**, *9*, 761−768.
(10) Wang, F.; Fang, R. H.; Luk, B. T.; Hu, C.-M. J.; Thamphiwatana, S.; Dehaini, D.; Angsantikul, P.; Kroll, A. V.; Pang, Z.; Gao, W.; Lu, W.; Zhang, L. Nanoparticle-Based Antivirulence Vaccine for the Management of Methicillin-Resistant *Staphylococcus aureus* Skin Infection. *Adv. Funct. Mater.* **2016**, *26*, 1628−1635.
(11) Khan, S. A.; Singh, A. K.; Senapati, D.; Fan, Z.; Ray, P. C. Nanomaterials for targeted detection and photothermal killing of bacteria. *Chem. Soc. Rev.* **2012**, *41*, 3193−3209.
(12) Huang, T.-C.; Lee, J.-F.; Chen, J.-Y. Pardaxin, an antimicrobial peptide, triggers caspase-dependent and ROS-mediated apoptosis in HT-1080 cells. *Mar. Drugs* **2011**, *9*, 1995−2009.
(13) Huang, H.-N.; Pan, C.-Y.; Chan, Y.-L.; Chen, J.-Y.; Wu, C.-J. Use of the antimicrobial peptide pardaxin (GE33) to protect against methicillin-resistant *Staphylococcus aureus* infection in mice with skin injuries. *Antimicrob. Agents Chemother.* **2014**, *58*, 1538−1545.
(14) Nellore, B. P. V.; Kanchanapally, R.; Pramanik, A.; Sinha, S. S.; Chavva, S. R.; Hamme, A.; Ray, P. C. Aptamer-Conjugated Graphene Oxide Membranes for Highly Efficient Capture and Accurate Identification of Multiple Types of Circulating Tumor Cells. *Bioconjugate Chem.* **2015**, *26*, 235−242.
(15) Pramanik, A.; Vangara, A.; Nellore, B. P. V.; Sinha, S. S.; Chavva, S. R.; Jones, S.; Ray, P. C. Development of Multifunctional Fluorescent-Magnetic Nanoprobes for Selective Capturing and Multicolor Imaging of Heterogeneous Circulating Tumor Cells. *ACS Appl. Mater. Interfaces* **2016**, *8*, 15076−15085.
(16) Fan, Z.; Shelton, M.; Singh, A. K.; Senapati, D.; Khan, S. A.; Ray, P. C. Multifunctional Plasmonic Shell−Magnetic Core Nanoparticles for Targeted Diagnostics, Isolation, and Photothermal Destruction of Tumor Cells. *ACS Nano* **2012**, *6*, 1065−1073.
(17) Hu, F.; Huang, Y.; Zhang, G.; Zhao, R.; Yang, H.; Zhang, D. Targeted Bioimaging and Photodynamic Therapy of Cancer Cells with an Activatable Red Fluorescent Bioprobe. *Anal. Chem.* **2014**, *86*, 7987−7995.
(18) Ding, H.; Yu, S.-B.; Wei, J.-S.; Xiong, H.-M. Full-Color Light-Emitting Carbon Dots with a Surface-State-Controlled Luminescence Mechanism. *ACS Nano* **2016**, *10*, 484−491.
(19) Meziani, M. J.; Dong, X.; Zhu, L.; Jones, L. P.; LeCroy, G. E.; Yang, F.; Wang, S.; Wang, P.; Zhao, Y.; Yang, L.; Tripp, R. A.; Sun, Y.-P. Visible-Light-Activated Bactericidal Functions of Carbon "Quantum" Dots. *ACS Appl. Mater. Interfaces* **2016**, *8*, 10761−10766.
(20) Wu, I.-C.; Yu, J.; Ye, F.; Rong, Y.; Gallina, M. E.; Fujimoto, B. S.; Zhang, Y.; Chan, Y.-H.; Sun, W.; Zhou, X.-H.; Wu, C.; Chiu, D. T. Squaraine-Based Polymer Dots with Narrow, Bright Near-Infrared Fluorescence for Biological Applications. *J. Am. Chem. Soc.* **2015**, *137*, 173−178.
(21) Liu, H.-Y.; Wu, P.-J.; Kuo, S.-Y.; Chen, C.-P.; Chang, E.-H.; Wu, C.-Y.; Chan, Y.-H. Quinoxaline-Based Polymer Dots with Ultrabright Red to Near-Infrared Fluorescence for in Vivo Biological Imaging. *J. Am. Chem. Soc.* **2015**, *137*, 10420−10429.
(22) Sun, Y.; Cao, W.; Li, S.; Jin, S.; Hu, K.; Hu, L.; Huang, Y.; Gao, X.; Wu, Y.; Liang, X.-J. Ultrabright and multicolorful fluorescence of amphiphilic polyethyleneimine polymer dots for efficiently combined imaging and therapy. *Sci. Rep.* **2013**, *3*, 3036.
(23) Baker, S. N.; Baker, G. A. Luminescent carbon nanodots: Emergent nanolights. *Angew. Chem., Int. Ed.* **2010**, *49*, 6726−6744.
(24) Bao, L.; Liu, C.; Zhang, Z.-L.; Pang, D.-W. Photoluminescence-Tunable Carbon Nanodots: Surface-State Energy-Gap Tuning. *Adv. Mater.* **2015**, *27*, 1663−1667.
(25) Pramanik, A.; Fan, Z.; Chavva, S. R.; Sinha, S. S.; Ray, P. C. Highly Efficient and Excitation Tunable Two-Photon Luminescence Platform for Targeted Multi-Color MDRB Imaging Using Graphene Oxide. *Sci. Rep.* **2014**, *4*, 6090.
(26) Jiang, K.; Sun, S.; Zhang, L.; Lu, Y.; Wu, A.; Cai, C.; Lin, H. Red, Green, and Blue Luminescence by Carbon Dots: Full-Color Emission Tuning and Multicolor Cellular Imaging. *Angew. Chem., Int. Ed.* **2015**, *54*, 5360−5363.
(27) Ye, R.; Xiang, C.; Lin, J.; Peng, Z.; Huang, K.; Yan, Z.; Cook, N. P.; Samuel, E. L. G.; Hwang, C.-C.; Ruan, G.; Ceriotti, G.; Raji, A.-R. O.; Marti, A. A.; Tour, J. M. Coal as an abundant source of graphene quantum dots. *Nat. Commun.* **2013**, *4*, 2943−2948.
(28) Liu, J.; Wickramaratne, N. P.; Qiao, S. Z.; Jaroniec, M. Molecular-Based Design and Emerging Applications of Nanoporous Carbon Spheres. *Nat. Mater.* **2015**, *14*, 763−774.
(29) Hu, S.; Trinchi, A.; Atkin, P.; Cole, I. Tunable Photoluminescence Across the Entire Visible Spectrum from Carbon Dots Excited by White Light. *Angew. Chem., Int. Ed.* **2015**, *54*, 2970−2974.
(30) Shi, Y.; Pramanik, A.; Tchounwou, C.; Pedraza, F.; Crouch, R. A.; Chavva, S. R.; Vangara, A.; Sinha, S. S.; Jones, S.; Sardar, D.; Hawker, C.; Ray, P. C. Multifunctional Biocompatible Graphene Oxide Quantum Dots Decorated Magnetic Nanoplatform for Efficient Capture and Two-Photon Imaging of Rare Tumor Cells. *ACS Appl. Mater. Interfaces* **2015**, *7*, 10935−10943.
(31) Lim, S. Y.; Shen, W.; Gao, Z. Carbon Quantum Dots and Their Applications. *Chem. Soc. Rev.* **2015**, *44*, 362−381.
(32) Fu, M.; Ehrat, F.; Wang, Y.; Milowska, K. Z.; Reckmeier, C.; Rogach, A. L.; Stolarczyk, J. K.; Urban, A. S.; Feldmann, J. Carbon Dots: A Unique Fluorescent Cocktail of Polycyclic Aromatic Hydrocarbons. *Nano Lett.* **2015**, *15*, 6030−6035.
(33) Zhang, X.; Chen, X.; Yang, J.; Jia, H.-R.; Li, Y.-H.; Chen, Z.; Wu, F.-G. Quaternized Silicon Nanoparticles with Polarity-Sensitive Fluorescence for Selectively Imaging and Killing Gram-Positive Bacteria. *Adv. Funct. Mater.* **2016**, *26*, 5958−5970.
(34) Crawford, S. E.; Andolina, C. M.; Smith, A. M.; Marbella, L. E.; Johnston, K. A.; Straney, P. J.; Hartmann, M. J.; Millstone, J. E. Ligand-Mediated "Turn On," High Quantum Yield Near-Infrared Emission in Small Gold Nanoparticles. *J. Am. Chem. Soc.* **2015**, *137*, 14423−14429.
(35) Wang, F.; Fang, R. H.; Luk, B. T.; Hu, C.-M. J.; Thamphiwatana, S.; Dehaini, D.; Angsantikul, P.; Kroll, A. V.; Pang, Z.; Gao, W.; Lu, W.; Zhang, L. Nanoparticle-Based Antivirulence Vaccine for the

DOI: 10.1021/acsomega.6b00518
ACS Omega 2017, 2, 554−562

Management of Methicillin-Resistant *Staphylococcus aureus* Skin Infection. *Adv. Funct. Mater.* **2016**, *26*, 1628−1635.
(36) Li, Y.-Q.; Zhu, B.; Li, Y.; Leow, W. R.; Goh, R.; Ma, B.; Fong, E.; Tang, M.; Chen, X. A Synergistic Capture Strategy for Enhanced Detection and Elimination of Bacteria. *Angew. Chem., Int. Ed.* **2014**, *53*, 5837−5841.
(37) Jones, S.; Sinha, S. S.; Pramanik, A.; Ray, P. C. Three-dimensional (3D) plasmonic hot spots for label-free sensing and effective photothermal killing of multiple drug resistant superbugs. *Nanoscale* **2016**, *8*, 18301−18308.
(38) Dai, X.; Fan, Z.; Lu, Y.; Ray, P. C. Multifunctional Nanoplatforms for Targeted Multidrug-Resistant-Bacteria Theranostic Applications. *ACS Appl. Mater. Interfaces* **2013**, *5*, 11348−11354.
(39) Kanchanapally, R.; Nellore, B. P. V.; Sinha, S. S.; Pedraza, F.; Jones, S. J.; Pramanik, A.; Chavva, S. R.; Tchounwou, C.; Shi, Y.; Vangara, A.; Sardar, D.; Ray, P. C. Antimicrobial Peptide-Conjugated Graphene Oxide Membrane for Efficient Removal and Effective Killing of Multiple Drug Resistant Bacteria. *RSC Adv.* **2015**, *5*, 18881−18887.
(40) Nellore, B. P. V.; Kanchanapally, R.; Pedraza, F.; Sinha, S. S.; Pramanik, A.; Hamme, A. T.; Arslan, Z.; Sardar, D.; Ray, P. C. Bio-Conjugated Cnt-Bridged 3D Porous Graphene Oxide Membrane for Highly Efficient Disinfection of Pathogenic Bacteria and Removal of Toxic Metals from Water. *ACS Appl. Mater. Interfaces* **2015**, *7*, 19210−19218.
(41) Meziani, M. J.; Dong, X.; Zhu, L.; Jones, L. P.; LeCroy, G. E.; Yang, F.; Wang, S.; Wang, P.; Zhao, Y.; Yang, L.; Tripp, R. A.; Sun, Y.-P. Visible-Light-Activated Bactericidal Functions of Carbon "Quantum" Dots. *ACS Appl. Mater. Interfaces* **2016**, *8*, 10761−10766.
(42) Reguera, J.; de Aberasturi, D. J.; Winckelmans, N.; Langer, J.; Bals, S.; Liz-Marzán, L. M. Synthesis of Janus Plasmonic−Magnetic, Star−Sphere Nanoparticles, and Their Application in SERS Detection. *Faraday Discuss.* **2016**, *191*, 47−59.
(43) Shi, D.; Sadat, M. E.; Dunn, A. W.; Mast, D. B. Photo-Fluorescent and Magnetic Properties of Iron Oxide Nanoparticles for Biomedical Applications. *Nanoscale* **2015**, *7*, 8209−8232.

DOI: 10.1021/acsomega.6b00518
ACS Omega 2017, 2, 554−562